fermentation

MDPI

Article

Synergistic Optimization of *Bacillus subtilis* for Efficiently Producing Menaquinone-7 (MK-7) by Atmospheric and Room Temperature Plasma (ARTP) Mutagenesis and Metabolic Engineering

Meng Li, Jiachang Li, Yufei Li, Xian Zhang and Jianzhong Xu *

The Key Laboratory of Industrial Biotechnology, Ministry of Education, School of Biotechnology, Jiangnan University, 1800 Lihu Road, Wuxi 214122, China; 15895357048@163.com (M.L.); ljc9421@126.com (J.L.); 1023210105@stu.jiangnan.edu.cn (Y.L.); zx@jiangnan.edu.cn (X.Z.)
* Correspondence: xujianzhong@jiangnan.edu.cn; Tel.: +86-510-85329312

Abstract: Menaquinone-7 (MK-7) plays a crucial role in preventing fractures and certain cardiovascular diseases and is one of the essential vitamins in the human body. In this study, a strain of *Bacillus subtilis* that produces MK-7 was isolated from commercially available natto fermentation agents, with an MK-7 titer of 75 mg/L. It was named L-5. Firstly, by employing Atmospheric and Room Temperature Plasma (ARTP) mutagenesis technology and protoplast fusion techniques, mutants resistant to 1-hydroxy-2-naphthoic acid (HNA) and diphenylamine (DPA) were obtained, with the titer of MK-7 reaching 196 mg/L. It was named R-8. Based on whole-genome sequencing technology, four mutants involved in the MK-7 synthesis pathway of strain L-5 were identified: 2-succinyl-5-enol-pyruvate-6-hydroxy-3-cyclohexen-1-carboxylic acid, MenD (S249L); (1,4)-dihydroxy-2-naphthalic acid-heptaisoprenyltransferase, MenA (S196L); 1-deoxy-D-xylose-5-phosphate synthetase, Dxs (N60D, Q185H); and hydroxy acid reductive isomerase, Dxr (Q351K). The overexpression of these mutants led to increases in MK-7 production of 19 mg/L, 20 mg/L, 17 mg/L, and 16 mg/L, respectively, compared to the unmutated genes. These mutations have been shown to be effective. To further enhance the production of MK-7, the mutants menD (S249L), menA (S196L), Dxs (N60D, Q185H), and Dxr (Q351K) were co-expressed. The final titer of MK-7 reached 239 mg/L. This study provides theoretical support for the future genetic modification of key enzymes in the MK-7 biosynthetic pathway.

Keywords: *Bacillus subtilis*; menaquinone-7; ARTP mutagenesis system; protoplast fusion; whole-genome sequencing; base mutation

check for updates

Academic Editors: Kaloyan Petrov and Penka Petrova

Received: 23 January 2025
Revised: 18 February 2025
Accepted: 20 February 2025
Published: 12 March 2025

Citation: Li, M.; Li, J.; Li, Y.; Zhang, X.; Xu, J. Synergistic Optimization of *Bacillus subtilis* for Efficiently Producing Menaquinone-7 (MK-7) by Atmospheric and Room Temperature Plasma (ARTP) Mutagenesis and Metabolic Engineering. *Fermentation* **2025**, *11*, 137. https://doi.org/10.3390/fermentation11030137

Copyright: © 2025 by the authors. Licensee MDPI, Basel, Switzerland. This article is an open access article distributed under the terms and conditions of the Creative Commons Attribution (CC BY) license (https://creativecommons.org/licenses/by/4.0/).

1. Introduction

Vitamin K2, also known as menaquinone (MK), is primarily produced through microbial metabolism. As a member of the vitamin K2 family, it is considered one of the fourth-generation drugs for osteoporosis treatment, offering significant potential in medical and food applications [1]. Additionally, vitamin K2 plays a crucial role as a key electron carrier in the respiratory chain [2], contributing to both electron transport and blood coagulation [3]. Vitamin K2 is not a single compound, but rather a family of compounds composed of several subtypes. Its chemical structure consists of a methylated naphthoquinone ring and a variable-length isoprenoid side chain. The number of units in the isoprenoid chain ranges from 1 to 14, with each variant denoted as MK-1 to MK-14 based on the number of isoprenoid units [4]. Among these subtypes, MK-7 is particularly notable

for its superior bioavailability and longer half-life compared to other forms of vitamin K2 [5].

Vitamin K2 was initially developed and used in Japan, primarily due to its presence in the traditional Japanese food natto, a fermented soybean dish that contains approximately 800–900 μg of vitamin K2 per 100 g [6]. With ongoing research, it was found that the primary fermentation strains in natto are *subtilis*, which not only produce fibrinolysin but also generate MK-7. While the extraction of MK-7 from natto remains an important method of obtaining this compound, its low titer poses a challenge for industrial-scale production. In recent years, in order to achieve higher production rates, researchers have identified various strains capable of producing MK-7 [7]. Among the strains, *Bacillus subtilis*, *Bacillus amyloliquefaciens*, and *Bacillus licheniformis* are considered the most promising candidates for MK-7 production. Notably, *Bacillus subtilis* is regarded as one of the most viable strains due to its rapid growth rate, genetic stability, and availability of extensive genetic modification tools. Therefore, *Bacillus subtilis* is considered one of the most promising species for large-scale MK-7 production [8]. The main strategies for improving MK-7 production focus on mutagenesis and metabolic engineering. Atmospheric and Room Temperature Plasma (ARTP) is an innovative and efficient biological breeding mutagenesis method. This system generates a plasma jet with a high concentration of reactive particles at atmospheric pressure and room temperature, representing a composite mutagenesis technique. Compared to traditional chemical or ultraviolet (UV) mutagenesis methods, ARTP mutagenesis offers several advantages, including safety, simplicity, and a high rate of positive mutations [9]. The metabolic biosynthesis pathway of MK-7 consists of four modules (Figure 1). In Module II, diphenylamine (DPA) inhibits the enzyme polyprenyl pyrophosphate synthetase in the MEP metabolic pathway, which regulates the synthesis of the isoprene side chain [10]. Additionally, 1,4-dihydroxy-2-naphthoic acid (DHNA) exerts feedback inhibition on DAHP synthase in Module III's shikimate pathway, an enzyme responsible for the formation of the quinone backbone. 1-Hydroxy-2-naphthoate (HNA), a structural analog of DHNA, is commonly used to screen for DHNA-resistant strains that produce higher titers of MK-7 [11]. Xu et al. applied Atmospheric Pressure Room Temperature plasma (ARTP) mutagenesis and protoplast fusion technology to wild-type *Bacillus amyloliquefaciens*, obtaining resistant mutant strains with various traits, including resistance to 1-hydroxy-2-naphthoic acid (HNA), sulfanilamide (SG), and menaquinone. The MK-7 titer reached 73.57 mg/L, which is 1.36 times higher than the parental strain [12]. In another study by Xu et al., ARTP mutagenesis was used to generate DPA-resistant mutant strains, resulting in enhanced MK-7 production [13]. MK-7, as a secondary metabolite, is involved in several metabolic pathways, including the glycerol metabolism pathway, the methylerythritol phosphate (MEP) pathway, the shikimate (SA) pathway, and the menaquinone biosynthesis pathway. The metabolic network is complex, involving numerous enzymes. Low expression levels of key enzymes in these pathways are a major factor limiting the MK-7 titer. MA et al. used *Bacillus subtilis* 168 as a chassis and overexpressed different combinations of rate-limiting enzymes, including Dxs, Dxr, IdI, and MenA, constructing 12 different *Bacillus subtilis* 168 strains. The best MK-7-producing strain achieved a titer of 50 mg/L, which is 11 times higher than the parental strain [14]. Yang et al. also used *Bacillus subtilis* 168 as a chassis for modular metabolic engineering design, dividing the MK-7 biosynthesis pathway into four modules. By overexpressing rate-limiting enzymes in different modules and knocking out metabolic branches, they obtained a strain that produced MK-7 with a titer of 69.5 mg/L [15]. Kong et al. overexpressed *menA* and *menD*, leading to a five-fold increase in MK-8 production compared to the wild-type *Escherichia coli* [16]. Although previous studies on mutagenesis and metabolic engineering have led to improvements in MK-7 production, the titers are still insufficient for industrial-scale production.

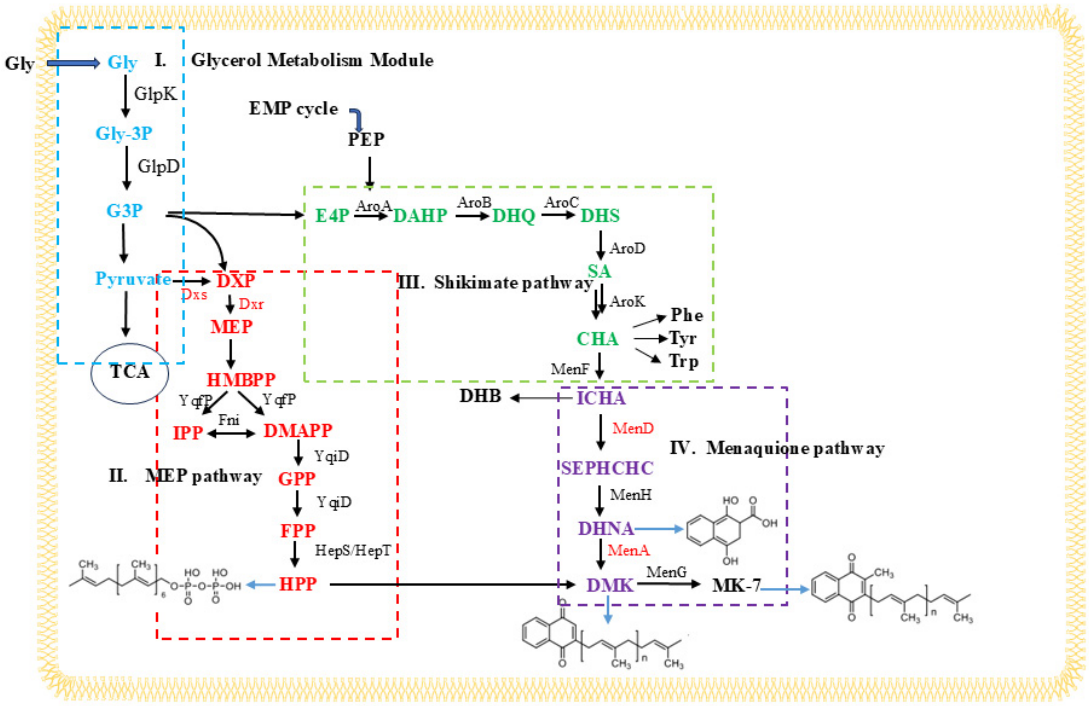


Figure 1. *Bacillus subtilis* MK-7 synthesis pathway [15]. Enzymes in the synthesis pathway: GlpK, glycerol kinase; GlpD, glycerol-3-phosphate dehydrogenase; AroA, 3-deoxy-D-arabinohepturate-7-phosphate synthetase; AroB, 3-dehydroquinic acid synthase; AroC, 3-dehydroquinic acid dehydrase; AroD, shikimic acid dehydrogenase; AroK, shikimic acid kinase; MenF, heterobranchic acid synthase; MenD, 2-succinyl-5-enol-pyruvate-6-hydroxy-3-cyclohexen-1-carboxylic acid synthetase; MenH, 2-succinyl-6-hydroxy-(2,4)-cyclohexadiene-1-carboxylate synthase; MenA, (1,4)-dihydroxy-2-naphthalic acid-heptaisoprenyltransferase; MenG, desmethylnaphthoquinone methyltransferase; Dxs, 1-deoxy-D-xylose-5-phosphate synthetase; Dxr, hydroxy acid reductive isomerase; YqfP, 4-hydroxy-3-methylbut-2-enyl diphosphate reductase; Fni, isoprenoid diphosphate isomerase; YqiD, farnesyl diphosphate synthase; HepS/HepT, heptaprenyl diphosphate synthase component I/II. Intermediate metabolites: Gly, glycerol; G3P, glyceraldehyde-3-phosphate; DXP, 1-deoxy-D-xylose-5-phosphate; MEP, 2-C-methyl-erythritol-4-phosphate; HMBPP, 1-hydroxy-2-methyl-2-butenyl-4-pyrophosphate; DMAPP, dimethylallyl diphosphate; IPP, isoprenyl diphosphate; GPP, geranyl diphosphate; FPP, farnesyl diphosphate; Hepta-PP, heptaisoprenylpyrophosphate; DAHP, dihydroxyacetone phosphate; E4P, erythrittose-4-phosphate; PEP, phosphoenolpyruvate; DHQ, 3-dehydroquinic acid; DHS, 3-dehydroshimate; SA, shikimic acid; CHA, chorismite; ICHA, isochorismate; DHB, 2,5-dihydroxyterephthalic acid; SEPHCHC, 2-succinyl-5-enol, pyruvoyl-6-hydroxy-3-cyclohexen-1-carboxylic acid; DHNA, 1,4-dihydroxy-2-naphthalenecarboxylic acid; DMK, desmenaquinone. MK-7, menaquinone-7. TCA, tricarboxylic acid cycle; EMP, glycolysis pathway.

The starting strain for this study was a wild-type *Bacillus subtilis* isolated from a natto fermentation agent, with an initial MK-7 production of 75.18 mg/L, which was designated as L-5. ARTP mutagenesis was performed to randomly mutate the strain, resulting in two MK-7-producing mutant strains with resistance to 1-hydroxy-2-naphthoic acid (HNA) and diphenylamine (DPA), named H-10 and D-15, with MK-7 titers of 175.55 mg/L and 164.49 mg/L, respectively. Subsequently, protoplast fusion technology was applied to fuse the H-10 and D-15 strains, generating the optimal fusion strain R-8, which produced 196.68 mg/L MK-7. Whole-genome sequencing and resequencing were performed on the R-8 strain and its parental L-5 strain, respectively. Subsequent sequence alignment between the two revealed mutations in key genes involved in the MK-7 biosynthesis pathway. Specifically, in the menaquinone biosynthesis pathway, the key enzyme MenD (succinyl-5-enolpyruvyl-6-hydroxy-3-cyclohexen-1-carboxylate synthase) showed a muta-

tion at position 249, where serine was replaced by leucine. Another rate-limiting enzyme, MenA (1,4-dihydroxy-2-naphthoic acid-7-isoprenyl transferase), exhibited a mutation at position 196, where serine was replaced by lysine. In the methylerythritol phosphate (MEP) pathway, the rate-limiting enzyme Dxs (1-deoxy-D-xylulose-5-phosphate synthase) had two mutations: asparagine at position 60 was replaced by aspartic acid, and glutamine at position 185 was replaced by histidine. Additionally, another rate-limiting enzyme, Dxr (hydroxyacid reductase isomerase), exhibited a mutation at position 351, where glutamine was replaced by lysine. The wild-type genes from the L-5 strain and the mutated genes from the R-8 strain were overexpressed in the R-8 strain. Overexpression of the *menD*, *menA*, *Dxs*, and *Dxr* genes from R-8 resulted in MK-7 titers that were 19.65 mg, 20.71 mg, 17.35 mg, and 16.28 mg higher, respectively, compared to the *menD*, *menA*, *Dxs*, and *Dxr* genes from the wild-type strain L-5. For each gene, overexpression of the mutant alleles resulted in higher titers than the wild-type, suggesting that these mutations in *menD*, *menA*, *Dxs*, and *Dxr* are beneficial, likely through enhanced enzyme activity or increased expression levels, thereby improving MK-7 production. To further increase the MK-7 titer, the *menD*, *menA*, *Dxs*, and *Dxr* genes were co-expressed, resulting in a final MK-7 titer of 239.65 mg/L. This study provides theoretical guidance for future modifications of key enzymes in the MK-7 biosynthetic pathway.

2. Materials and Methods

2.1. Experimental Materials

Natto Fermentation Agent Samples: A total of 10 samples from different provinces and manufacturers in China were collected. The manufacturers included the following: T manufacturer (Sweet Kitchen, Beijing, China), H manufacturer (Podikai Health Food Exclusive Online Store, Changzhou, China), S manufacturer (Chuanxiu Flagship Store, Langfang, China), R manufacturer (Hao Ding Food Speciality, Chongqing, China), L manufacturer (Tangdoudou Snack House, Zhaoqing, China), Q manufacturer (Nongjian Flagship Store, Anqing, China), D manufacturer (Yongyuan Food Ferment, Ningde, China), J manufacturer (Yinuan Food Flagship Store, Sanming, China), Y manufacturer (Baisenyou Food Flagship Store, Shanghai, China) and W manufacturer (Runwanxiang Seasoning Shop, Dezhou, China).

2.2. Strains and Plasmids

In this study, *Escherichia coli* JM110 was used for DNA fragment amplification, plasmid construction, and plasmid storage. The strains and plasmids used and constructed in this study are listed in Table 1. The primers used in this study are listed in Supplementary S1.2, Table S1.

Table 1. The main strains and plasmids used in this study.

Strain and Plasmid	Description	Source
Strain		
Escherichia coli JM110	Cloning host	Beyotime
L-5	Wild-type *Bacillus subtilis*	This study
H-10	1-Hydroxy-2-naphthoic acid resistance mutant	This study
D-15	Diphenylamine resistance mutant	This study
R-8	Diphenylamine and 1-hydroxy-2-naphthoic acid resistance mutant	This study

Table 1. *Cont.*

Strain and Plasmid	Description	Source
R-81	Strain R-8 harboring the pMA5-*menD*^{WT}	This study
R-82	Strain R-8 harboring the pMA5-*menA*^{WT}	This study
R-83	Strain R-8 harboring the pMA5-*Dxs*^{WT}	This study
R-84	Strain R-8 harboring the pMA5-*Dxr*^{WT}	This study
R-85	Strain R-8 harboring the pMA5-*menD*^{MT}	This study
R-86	Strain R-8 harboring the pMA5-*menA*^{MT}	This study
R-87	Strain R-8 harboring the pMA5-*Dxs*^{MT}	This study
R-88	Strain R-8 harboring the pMA5-*Dxr*^{MT}	This study
R-89	Strain R-8 harboring the pMA5-*menA-menD-Dxs-Dxr*^{MT}	This study
Plasmid		
pMA5	The pMA5 is an *E. coli/B. subtilis* shuttle plasmid that is mainly used for protein expression in *B. subtilis*. Amp^{r} Km^{r}	Thermo Fisher Scientific
pMA5-*menD*^{WT}	pMA5 with *menD*, in which the gene *menD* is derived from the wild-type strain L-5	This study
pMA5-*menA*^{WT}	pMA5 with *menA*, in which the gene *menA* is derived from the wild-type strain L-5	This study
pMA5-*Dxs*^{WT}	pMA5 with *Dxs*, in which the gene *Dxs* is derived from the wild-type strain L-5	This study
pMA5-*Dxr*^{WT}	pMA5 with *Dxr*, in which the gene *Dxr* is derived from the wild-type strain L-5	This study
pMA5-*menD*^{MT}	pMA5 with *menD*, in which the gene *menD* is derived from the mutant strain R-8	This study
pMA5-*menA*^{MT}	pMA5 with *menA*, in which the gene *menA* is derived from the mutant strain R-8	This study
pMA5-*Dxs*^{MT}	pMA5 with *Dxs*, in which the gene *Dxs* is derived from the mutant strain R-8	This study
pMA5-*Dxr*^{MT}	pMA5 with *Dxr*, in which the gene *Dxr* is derived from the mutant strain R-8	This study
pMA5-*menA-menD-Dxs-Dxr*^{MT}	pMA5 with *menA*, *menD*, *Dxs*, and *Dxr*, in which the genes *menA*, *menD*, *Dxs*, and *Dxr* are derived from the mutant strain R-8	This study

2.3. Media and Cultivation Conditions

2.3.1. Media

Basic Isolation Medium (g/L): Glucose 15, Soybean peptone 15, Fibrinogen 5, $KH_2PO_4 \cdot 12H_2O$ 1, $K_2HPO_4 \cdot 3H_2O$ 2.5, $MgSO_4 \cdot 7H_2O$ 2.5, Streptomycin 0.5, Agar 15, pH 7.0–7.2.

Luria-Bertani (LB) Medium (g/L): Tryptone 10, Yeast extract 5, NaCl 10, pH 7.0.

Seed Culture Medium (g/L): Glucose 15, Soybean peptone 15, $K_2HPO_4 \cdot 3H_2O$ 2.5, KH_2PO_4 1.5, $MgSO_4 \cdot 7H_2O$ 2.5, pH 7.0.

Fermentation Medium (g/L): Glycerol 50, Soybean peptone 100, NaCl 3, K_2HPO_4 6, pH 7.0–7.3.

Regeneration Medium (g/L): Tryptone 10, Yeast extract 5, Beef extract 5, KH_2PO_4 1.5, $K_2HPO_4 \cdot 3H_2O$ 4.6, NaCl 40.28, Maleic acid 2.32, $MgCl_2$ 1.9, pH 7.0.

All media, with the exception of the fermentation medium that was subjected to autoclaving at 115 °C for 10 min, were sterilized at 121 °C for 20 min.

2.3.2. Main Solutions

Hypertonic Buffer (SMM Buffer): Sucrose 0.5 mol·L^{-1}, Maleic acid 20 mmol·L^{-1}, $MgCl_2$ 20 mmol·L^{-1}, pH 6.5.

Lysozyme Buffer (0.1 mg·mL^{-1}): Dissolve 1 mg of lysozyme (activity $\geq$ 20,000 U·mg^{-1}) in 10 mL of SMM buffer.

PEG6000 Buffer: Dissolve 4 g of PEG6000 in SMM buffer and adjust the final volume to 10 mL.

The sterilization conditions for both the Hypertonic Buffer (SMM Buffer) and the PEG6000 Buffer were autoclaving at 121 °C for 20 min, and the Lysozyme Buffer was sterilized by filtration.

2.3.3. Cultivation Methods

Shake Flask Culture: After activation (inoculate 100 µL of the strain preserved in glycerol stock into a 100 mL conical flask containing 10 mL of liquid LB medium), 600 µL of the wild-type *Bacillus subtilis* was inoculated into a 250 mL Erlenmeyer flask containing 30 mL of LB medium. The culture was incubated at 37 °C with shaking at 220 rpm during the exponential growth phase for subsequent mutagenesis.

Shake Flask Fermentation: After activation (inoculate 100 µL of the strain preserved in glycerol stock into a 100 mL conical flask containing 10 mL of liquid LB medium), 300 µL of the mutated and selected strain was inoculated into a 250 mL Erlenmeyer flask containing 30 mL of seed culture medium. The culture was incubated at 37 °C with shaking at 220 rpm for 10 h. Then, 600 µL of the seed culture was inoculated into a 250 mL Erlenmeyer flask containing 30 mL of fermentation medium and incubated at 37 °C with shaking at 220 rpm for 6 days before sampling and analysis.

2.4. Isolation and Screening of Wild-Type Bacillus subtilis for MK-7 Production

Five grams of each of the ten natto fermentation agent samples mentioned above was dissolved in 20 mL of sterile water and subjected to a 10 min incubation in a water bath at 85 °C. The mixture was then centrifuged at 5000 rpm for 10 min, and the supernatant was collected. After appropriate dilution, the supernatant was plated on initial screening plates. The plates were incubated at 37 °C for 24 h. Strains with larger clear zones were selected for further shake flask fermentation to validate MK-7 production. One high-yield strain was ultimately selected.

To identify the isolated MK-7-producing strain, we followed the procedures described in the Bergey's Manual of Determinative Bacteriology [17]. The strain was subjected to morphological, physiological, and biochemical identification. Genomic DNA of the isolated strain was extracted using the Genomic DNA Extraction Kit from Nanjing China Genewiz. The 16S rRNA gene was amplified using universal bacterial primers (F: 5′ GAGAGTTTGATCCTGGCTCAG-3′; R: 5′ CTACGGCTACCTTGTTACGA-3′) via PCR. The PCR conditions were as follows: pre-denaturation at 95 °C for 5 min, denaturation at 95 °C for 30 s, annealing at 56 °C for 30 s, extension at 72 °C for 90 s, and a final extension at 72 °C for 10 min. This cycle was repeated 30 times. The purified PCR products were then sent to Shanghai Sheng gong Biotechnology Co., Ltd. (Shanghai, China) for sequencing.

2.5. ARTP Mutagenesis

To initiate ARTP mutagenesis, 1 mL of the parent strain cultured to the exponential phase was centrifuged at 5000 rpm, and the supernatant was discarded. The cell pellet was washed three times with saline solution containing 5% glycerol and resuspended. A 10 µL aliquot of the resuspended cells was then spread on a metal plate for mutagenesis treatment. The ARTP-IIS mutagenesis (Wuxi TMAXTREE Biotechnology Co. Ltd., Wuxi,

China) device was used to perform random mutagenesis on the strain. The mutagenesis protocol, based on prior studies [18] with minor modifications, was set as follows: incident power of 100 W, gas flow rate of 10 SLM, and the distance between the sample and the plasma nozzle was maintained at 2 mm. The mutagenesis treatment lasted for 90 s. After mutagenesis, the metal plate was placed in a 1.5 mL centrifuge tube containing 990 μL of physiological saline. The mixture was vortexed for at least one minute to elute the mutagenized cells from the plate into the saline solution. The eluate was then diluted appropriately and spread on LB solid agar plates containing HNA and DPA. The plates were incubated at 37 °C for 24 to 36 h. Colonies with larger diameters were selected, and each colony was subjected to shake flask fermentation validation with three replicates.

2.6. Protoplast Fusion

The protoplast fusion method used in this study was adapted from the previous literature with minor modifications [19]. Initially, two parental strains were inoculated into 10 mL of LB liquid medium and cultured overnight at 37 °C. Subsequently, 1 mL of the culture was transferred to 100 mL of LB medium and cultured at 37 °C until the logarithmic phase was reached. The culture was centrifuged at 5000 rpm for 10 min, and the supernatant was discarded. The cell pellet was washed twice with SMM solution, and the cells were resuspended in SMM containing 0.1 mg/mL lysozyme to an OD_{600} of 0.8. The suspension was then incubated at 8 °C for 20 min in a water bath. Under a microscope, the morphological change from rod-shaped to spherical cells was observed to confirm successful protoplast preparation. The successfully prepared protoplasts were washed twice with SMM, centrifuged, and resuspended.

Next, 2 mL of protoplasts from each of the two parent strains was combined and incubated for 5 min before centrifugation. A total of 1.8 mL of pre-warmed (42 °C) 40% PEG6000 and 0.2 mL of 0.2 mol/L $CaCl_2$ solution were added to resuspend the protoplasts. The mixture was then incubated in a 37 °C water bath for 10 min with gentle shaking. After the incubation, the protoplasts were collected by centrifugation at 4000 rpm for 15 min, washed twice with SMM, and resuspended in 1 mL of SMM. The protoplast suspension was appropriately diluted and spread onto regeneration medium plates. The plates were incubated at 37 °C for 12 to 24 h.

Finally, colonies that grew on the regeneration medium were harvested by washing the plate with SMM solution and then transferred onto selective plates containing HNA and DPA for screening protoplast fusion strains resistant to both HNA and DPA. Colonies with larger diameters were selected, and each colony was subjected to shake flask fermentation validation with three replicates.

2.7. Whole-Genome Sequencing of Wild-Type Bacillus subtilis

The successfully fused resistant mutant strains were inoculated into 10 mL of liquid LB medium and cultured at 37 °C with shaking at 200 rpm until the exponential growth phase was reached. The cells were collected by centrifugation at 3000 rpm for 5–10 min using a refrigerated centrifuge. The total cell pellet mass was approximately 1–2 g. The cell pellet was gently washed 1–2 times with pre-chilled PBS under sterile conditions to avoid contamination. After washing, the samples were either snap-frozen in liquid nitrogen or stored at −80 °C. The samples were shipped on dry ice to Jinwei BioTech (Nanjing, China) for whole-genome sequencing. Sequencing was performed using Illumina second-generation sequencing technology and the PacBio third-generation high-throughput sequencing platform. The obtained genomic sequence data were analyzed and annotated using databases including COG (COG-NCBI, accessed on 27 November 2024), GO (Gene Ontology Resource, accessed on 27 November 2024), KEGG (KEGG: Kyoto Encyclopedia of Genes and

Genomes, accessed on 28 November 2024), CAZY (CAZy-Home, accessed on 27 November 2024), CARD (The Comprehensive Antibiotic Resistance Database, accessed on 28 November 2024), and VFDB (Validated Antibody Database, antibodies, siRNA/shRNA, ELISA, cDNA clones, proteins/peptides, and biochemicals, accessed on 28 November 2024) to predict genes and annotate their functions.

2.8. Fibrinolytic Enzyme Activity Assay

The method for determining fibrinolytic enzyme activity was adapted from the literature [20]. Specifically, 20 µL of the sample was spotted onto a solid separation agar plate and incubated at 37 °C for 12 h. The diameter of the clear zone formed around the sample was then measured. Fibrinolytic enzyme activity was calculated by constructing a standard curve using urokinase, and the enzyme activity (IU/mL) of the fibrinolytic enzyme was determined by comparison with the urokinase units.

2.9. Analytical Method

The method for detecting MK-7 in the fermentation broth was adapted from the literature with slight modifications [21]. A total of 15 mL of extraction solvent (n-hexane:isopropanol in a 2:1 volume ratio) was added to 30 mL of fermentation broth after 6 days of fermentation. The mixture was then extracted for 12 h under dark conditions at 16 °C and 200 rpm. After extraction, the solution was centrifuged to collect the extract for further analysis. The extract was analyzed using high-performance liquid chromatography (HPLC) equipped with a UV detector. A C18 column (250 mm × 4.6 mm, 5 µm) was used, with methanol:dichloromethane (9:1, *v*/*v*) as the mobile phase, a flow rate of 1 mL/min, and a column temperature of 40 °C. Detection was carried out at a wavelength of 248 nm. Under the aforementioned conditions, the MK-7 standards with concentrations of 100 mg/L, 80 mg/L, 60 mg/L, 40 mg/L, and 20 mg/L were individually subjected to detection. Based on the peak areas obtained from the detection, the standard curve for MK-7 was determined to be y = 14.285x + 11.9 (R^2 = 0.9998), where x denotes the concentration of MK-7 and y represents the peak area value.

3. Results and Discussion

3.1. Isolation and Identification of MK-7-Producing Strains

- Six strains with large transparent zones were selected and named L-1, L-2, L-3, L-4, L-5, and L-6. The diameters of the transparent zones were measured, and each of these six strains was inoculated into fermentation medium. The fibrinolytic activity and MK-7 synthesis capability of the strains were calculated based on the standard curves for urokinase and MK-7, respectively. The results are shown in Table 2. The strain with the highest MK-7 production, L-5, was selected for subsequent experiments.

Table 2. Urokinase activity and MK-7 titer of the isolated strains.

Sample Name	L-1	L-2	L-3	L-4	L-5	L-6
Urokinase activity (IU/mL)	628.48 ± 3.6	566.59 ± 4.3	592.89 ± 6.8	628.48 ± 5.9	646.49 ± 3.2	584.09 ± 3.1
MK-7 titer (mg/L)	45.01 ± 0.23	68.64 ± 0.16	64.05 ± 0.30	53.38 ± 0.19	75.18 ± 0.42	44.07 ± 0.34

- The isolated high-titer strain was streaked onto LB agar plates and incubated at 37 °C for 12 h to observe colony characteristics. The colony surface was rough, opaque, and white or slightly yellow, with wrinkles forming around the colony after another 12 h of incubation (Figure 2A). When inoculated into liquid culture and

incubated at 37 °C for 12 h, the culture exhibited a characteristic foul odor reminiscent of rotten eggs. Gram staining indicated that the strain was Gram-positive, and microscopic examination revealed rod-shaped bacteria (Figure 2B). Physiological and biochemical identification of the strain was performed, and the results are summarized in Table 3. Based on the physiological and biochemical characteristics, and in comparison with the Bergey's Manual of Determinative Bacteriology and the Manual of Common Bacteria Identification, the strain was preliminarily identified as *Bacillus subtilis*.

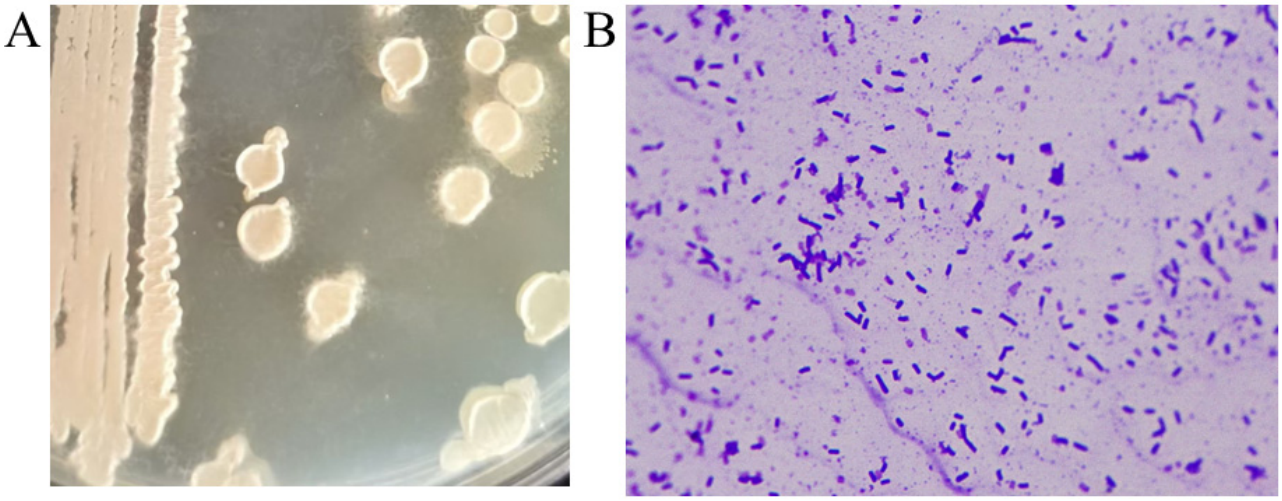


Figure 2. Identification of the isolated strains. (**A**) Colony morphology of the L-5 strain on agar plate culture medium; (**B**) Morphology of the L-5 strain under an optical microscope after Gram staining (Oil immersion lens 100 × 10 magnification).

Table 3. Physiological and biochemical experiments.

Experimental Project	Result
Voges–Proskauer (V-P) test	+
Lactose	-
Glucose	+
Maltose	+
Sucrose	+
Mannitol	-
Hydrogen sulfide production test	-

- The 16S rRNA sequencing results are presented in Supplementary S1.1, with a total sequence length of 1465 bp. The sequence was compared with the NCBI database, and a phylogenetic tree was constructed using the MEGA11 software (Figure 3). The results indicated that the isolated strain L-5 clustered in the same branch as *Bacillus subtilis* 168, with a close phylogenetic relationship. Based on the morphological characteristics of the bacteria, colony morphology, growth behavior on media, and the results from both morphological and biochemical identifications, the strain was confirmed to be *Bacillus subtilis*.

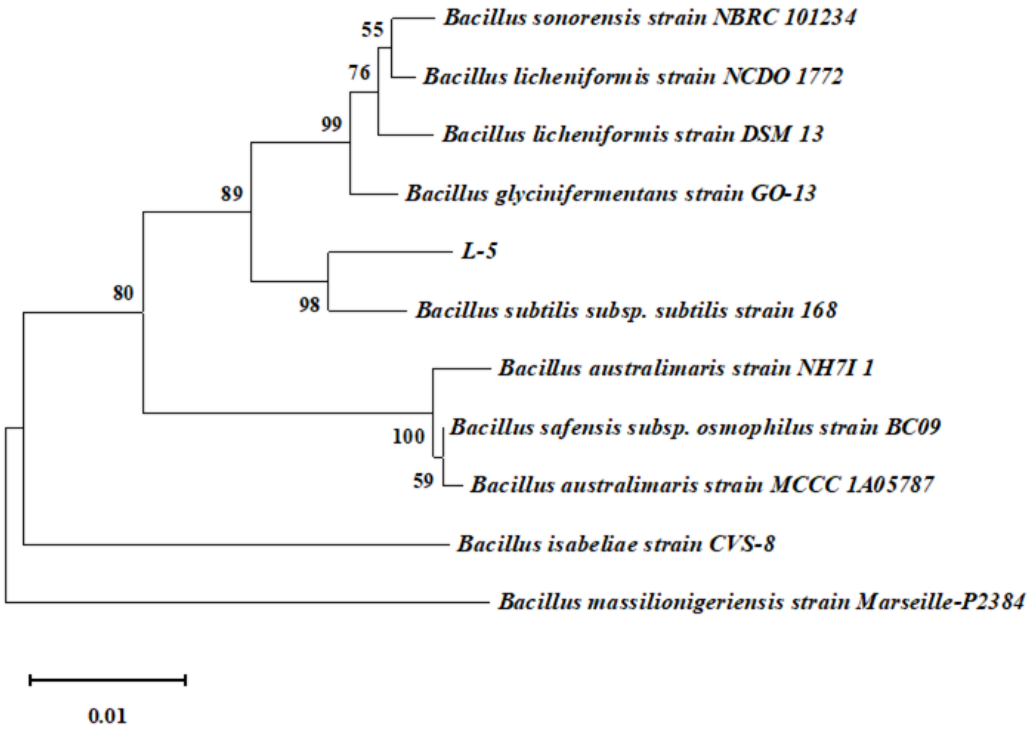


Figure 3. The phylogenetic tree constructed based on the 16S rRNA sequencing results of strain L-5.

3.2. Screening of the MK-7-Producing Strain for Resistance to HNA or DPA by ARTP

Mutant strains were selected by plating the mutated strains onto LB agar plates containing selective antibiotics. The concentration of HNA used for screening resistance mutants was gradually increased from 200 mg/L to 320 mg/L, and the concentration of DPA was raised from 50 mg/L to 90 mg/L. However, when the HNA concentration exceeded 270 mg/L, an inverse relationship was observed: as the HNA concentration increased, the MK-7 production of the resistant mutants decreased. Similarly, when the DPA concentration was increased beyond 75 mg/L, a comparable decrease in MK-7 production was noted. Upon analyzing the MK-7 production data from mutants selected at HNA concentrations ranging from 200 mg/L to 320 mg/L and DPA concentrations ranging from 50 mg/L to 90 mg/L, the optimal MK-7 production was observed at HNA 265 mg/L and DPA 65 mg/L.

Thus, in this study, mutant strains were specifically selected on LB antibiotic plates containing HNA at 265 mg/L and DPA at 75 mg/L. For each selective plate, 20 larger single colonies were picked for flask fermentation to verify MK-7 production. The results showed that 20 HNA-resistant mutants were obtained from the LB plates containing 265 mg/L HNA, with the best mutant, H-10 (Figure 4A), producing 175.55 mg/L MK-7, which is 2.28 times higher than the parent strain L-5. Similarly, 20 DPA-resistant mutants were selected from LB plates containing 75 mg/L DPA, with the best mutant, D-15 (Figure 4B), producing 164.49 mg/L MK-7, which is 2.04 times higher than the parent strain L-5. This study demonstrates that ARTP mutation is an effective method for obtaining high-titer MK-7 strains.

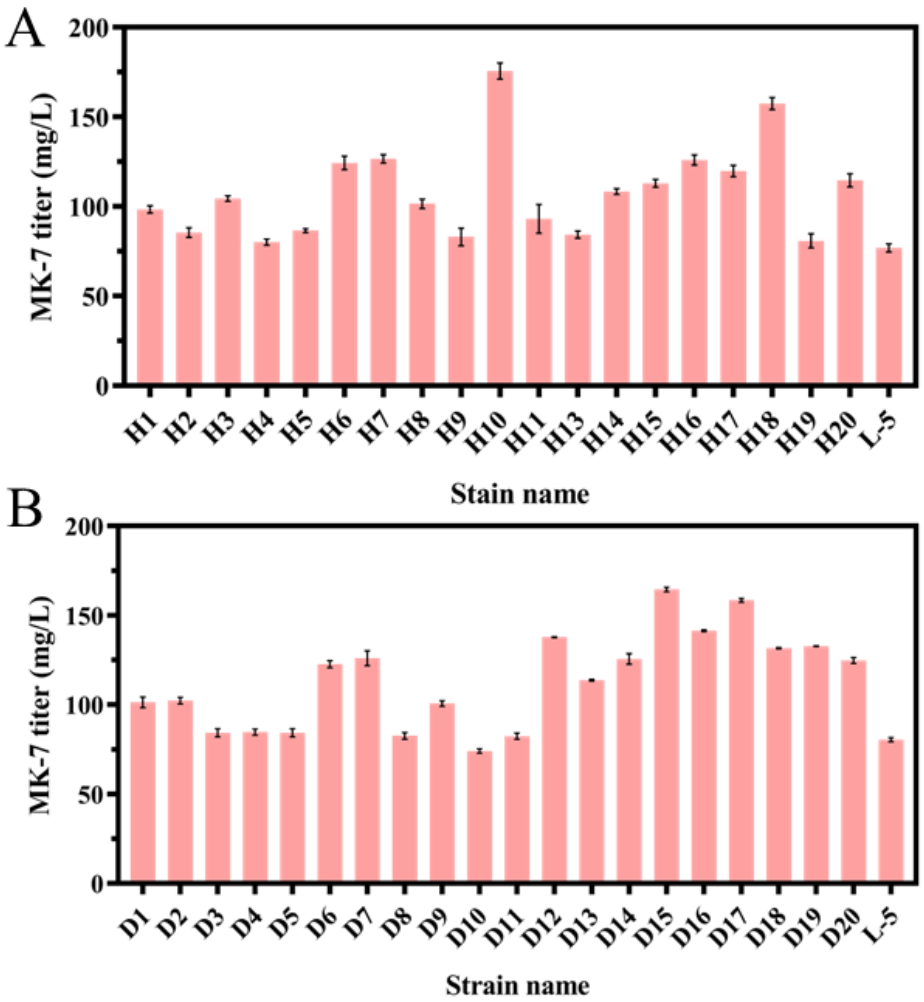


Figure 4. MK-7 production of parental strain and mutants with different genetic markers. Each strain was fermented independently three times. (**A**) MK-7 production of mutants with HNA (265 mg/L) resistance, where the maximum value of the standard deviation shown in the figure is 5.63 (mg/L). (**B**) MK-7 production of mutants with DPA (75 mg/L) resistance, where the maximum value of the standard deviation shown in the figure is 2.95 (mg/L).

3.3. Screening of the MK-7-Producing Strain for Resistance to HNA and DPA by Protoplast Fusion

The best HNA-resistant mutant H-10 obtained by ARTP mutagenesis was spread on an LB plate containing DPA (75 mg/L); the best DPA-resistant mutant D-15 was spread on an LB plate containing HNA (265 mg/L); both were cultured at 37 °C for 24 h, and no colonies grew. The results (Figure 5A) showed that H-10 did not have DPA resistance and that D-15 did not have HNA resistance. Chen's study demonstrated that protoplast fusion technology can be used to obtain fusion strains with multiple mutant genetic traits, thereby achieving high titers of surfactants [19]. In this study, to obtain higher titers of MK-7, the HNA-resistant mutant strain H-10 and the DPA-resistant mutant strain D-15 were selected as parental strains for protoplast fusion (Figure 5B). The goal was to generate strains with dual resistance mutations that could produce higher amounts of MK-7. After successful protoplast fusion, 11 larger colonies were selected for flask fermentation to verify MK-7 production. The results showed that the best fusion strain, R8 (Figure 5C), produced 196.68 ± 1.95 mg/L MK-7, which represents a 19.56% increase in MK-7 production compared to the parent strain D-15. Protoplast fusion of ARTP-mutated strains effectively enhanced MK-7 production. Strain R8 was selected as the strain for subsequent studies.

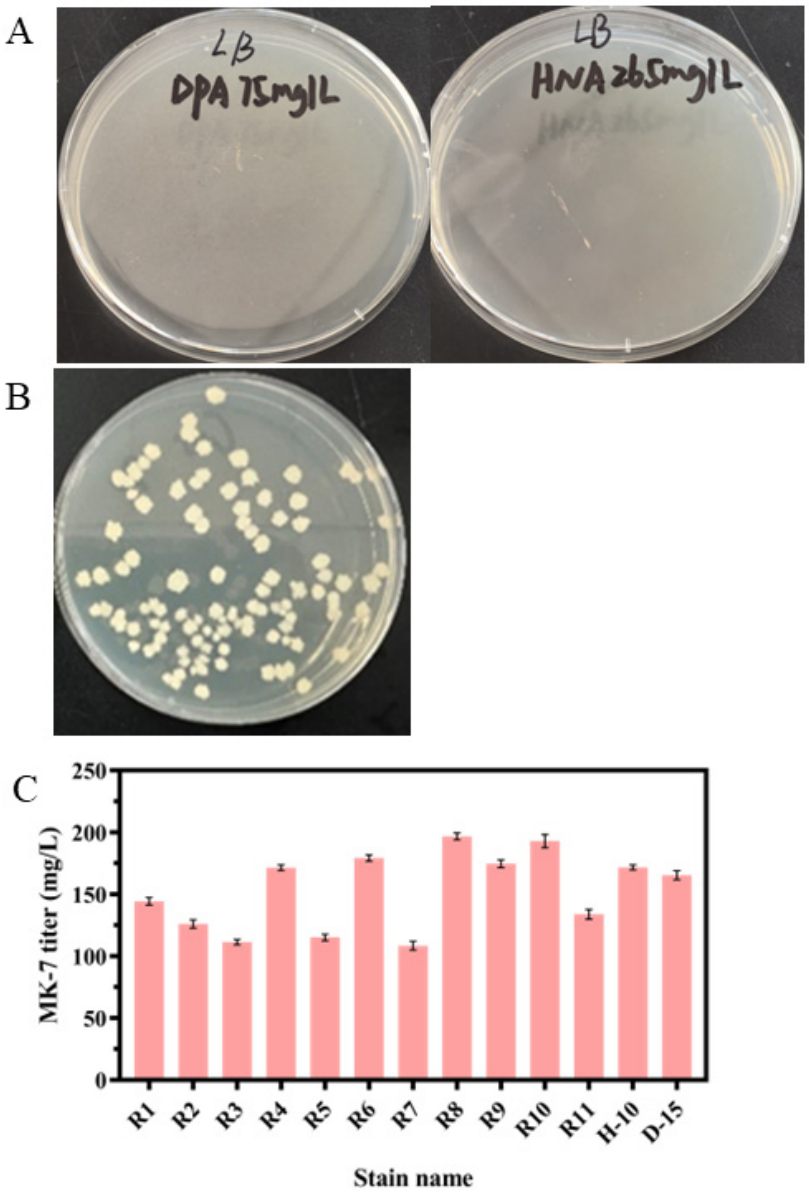


Figure 5. (**A**) Verification of whether the best HNA-resistant mutant H-10 has DPA (75 mg/L) resistance; verification of whether the best DPA-resistant mutant D-15 has HNA (265 mg/L) resistance. (**B**) HNA (265 mg/L) and DPA (75 mg/L) fusion strains. (**C**) MK-7 production of parental strain and fusion strains obtained from the protoplast fusion between the HNA-resistant mutant and DPA-resistant mutant, where the maximum value of the standard deviation shown in the figure is 3.81 (mg/L). Each strain was fermented independently three times.

3.4. Genomic Analysis and Identification of Key Gene Mutations

Currently, whole-genome sequencing (WGS) and genomic resequencing technologies are widely used as efficient tools for microbial identification, classification, and gene function analysis. These techniques also assist researchers in identifying potential mechanisms underlying beneficial mutations in mutant strains. Jiang et al. discovered through whole-genome sequencing and genomic analysis that defects in regulatory factors may affect the biosynthesis and accumulation of MK-7 by altering overall metabolic levels [22]. Min et al., based on whole-genome sequencing and transcriptomic analysis, discovered the mechanisms behind the over-accumulation of MK-7 in *Bacillus subtilis* [23]. In this study, whole-genome sequencing and genomic resequencing were performed on strains R-8 and L-5. The sequencing (Figure 6A) results revealed a 3,622,722 bp single circular chromo-

some with a GC content of 46.94%. A total of 4020 coding genes were predicted, along with 200 non-coding RNAs, which included 87 tRNA genes, 27 rRNAs, and 86 ncRNAs. Functional annotation was performed in the NR, KEGG, GO, COG, CAZy, Pfam, Swiss-Prot, CARD, and VFDB databases, resulting in the identification of 4015, 2660, 2383, 2981, 429, 3429, 3641, 267, and 4 functional genes, respectively. This paper presents a detailed gene functional annotation of strain R-8 using the three commonly used databases: COG, GO, and KEGG. According to the annotation results from the COG database (Figure 6B), excluding the categories "General function prediction only" and "Function unknown", the largest number of annotated genes were associated with "Amino acid transport and metabolism", followed by "Transcription", and "Carbohydrate transport and metabolism". These annotation results suggest that strain R-8 possesses robust capabilities for protein synthesis and transport, gene expression, and carbohydrate metabolism. The GO annotation results for strain R-8 are summarized in Figure 7A. The results demonstrated that GO items associated with "Catalytic activity" and "Metabolic processes" were the most prevalent. In this study, gene annotation was further performed in the KEGG pathway database. A total of 2660 genes were annotated and classified into 39 metabolic pathways (Figure 7B). The primary biological metabolic pathways of strain R-8 are concentrated in the "Metabolism" category. The key pathways include "Carbohydrate metabolism", "Global and overview maps", and "Amino acid metabolism", which are crucial biological processes. These robust metabolic pathways provide the energy necessary for efficient MK-7 synthesis. Additionally, the fourth-ranked pathway involves the "Metabolism of cofactors and vitamins", with 182 associated genes. This indicates that vitamin metabolism pathways in R-8 should not be overlooked, and mutations in related genes may be a significant factor contributing to the increased MK-7 titer.

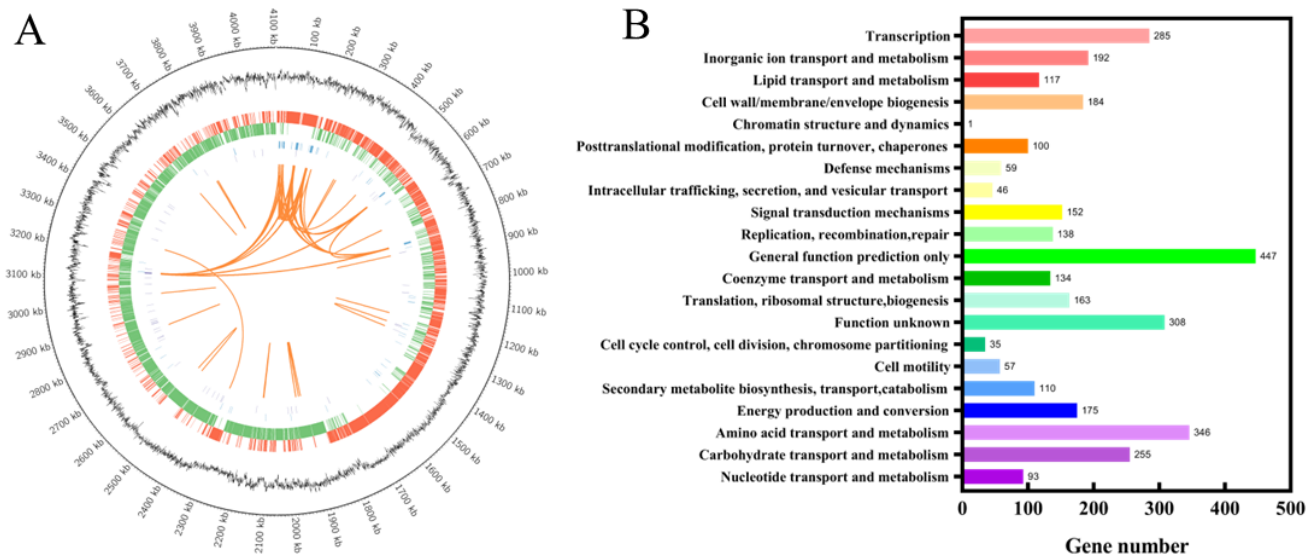


Figure 6. The gene circle map of R-8 and COG gene annotation. (**A**) Figure legend: The circular diagram displays seven types of information. From the outermost to the innermost circles, the first circle represents genomic location information; the second circle represents GC content information; the third circle represents coding genes on the positive strand (marked in red); the fourth circle represents coding genes on the negative strand (marked in green); the fifth circle represents ncRNA information on the positive strand (marked in blue); the sixth circle represents ncRNA information on the negative strand (marked in purple); the seventh circle represents long-segment repeat sequence information within the genome (marked in orange). (**B**) COG functional classification of genes. The horizontal axis represents the number of annotated COG genes in each category, and the vertical axis represents the explanation for each category.

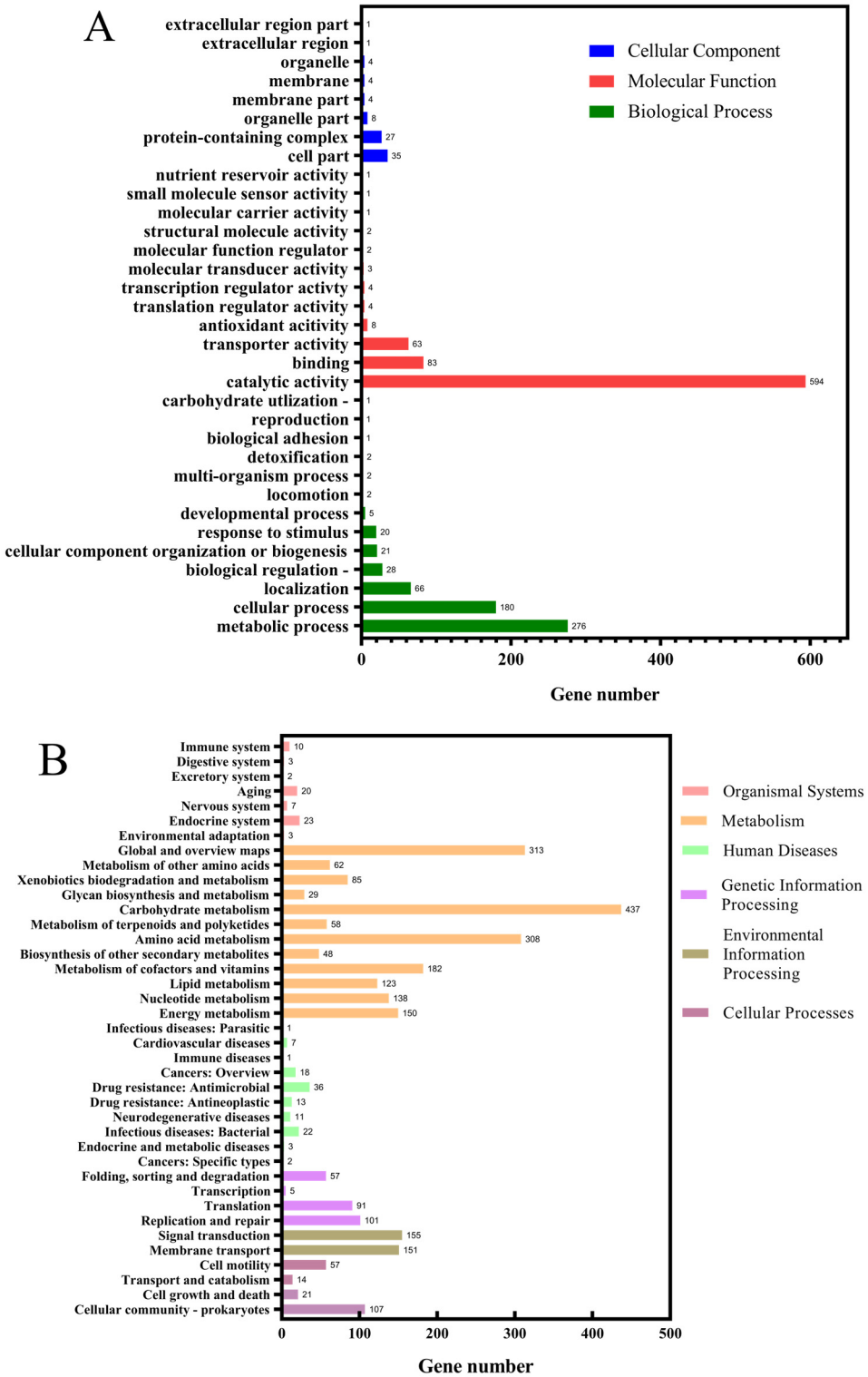


Figure 7. Gene function annotation. (**A**) GO items. The vertical axis represents the GO term; the horizontal axis represents the number of genes; different colors are used to distinguish biological processes, cellular components, and molecular functions. (**B**) KEGG pathway map. The vertical axis represents the secondary classification of biological pathways; the horizontal axis represents the number of genes; different colors are used to distinguish the primary classification of biological pathways.

Previous studies have shown that the enzymes Dxs, Dxr, GlpD, MenA [15], MenD [24], MenB, MenG [25], Fni, and AroA [26] play key roles in the synthesis of MK-7 in *Bacillus subtilis*. This study focused specifically on the MK-7 biosynthetic pathway to identify genetic factors directly associated with the increased MK-7 production. The results (Table 4)

show that base changes occurred in four key enzyme genes involved in the production pathway. Among them, MenD, the key enzyme in the menaquinone synthesis pathway, had a mutation at amino acid position 249, where serine was substituted by leucine (Supplementary S1.3, Figure S1A). MenD is the first enzyme in the menaquinone synthesis pathway, competing with DhbB for the same precursor, isochorismate. Previous studies have shown that overexpressing the key genes *menA* or *menD* can enhance the substrate supply in the synthetic pathway, increasing the titer of MK-8 to about five times that of the parent strain [16]. In this study, the amino acid change at this site may enhance the enzyme activity of MenD, improving its competitive ability for isochorismate and enhancing the supply of the precursor substance, chorismite, and thereby directing more isochorismate towards menaquinone synthesis. Another rate-limiting enzyme in this pathway, MenA, a (1,4)-dihydroxy-2-naphthoic acid-7-isopentenyl transferase, also showed a mutation at amino acid position 196, where serine was substituted by lysine (Supplementary S1.3, Figure S1B). In Liu et al.'s study, site-directed mutations in the MenA and UbiA of the MK-7 biosynthesis pathway enhanced the expression of MenA while reducing the mRNA and protein expression of UbiA, resulting in a decrease in the ubiquinone (UQ) concentration and increased MK-7 production. Their research suggests that mutations in key enzymes of the MK-7 pathway could be a significant factor in the increased MK-7 titer [27]. This indicates that site-directed mutation of MenA can obtain effective mutants, increasing the titer of MK-7. In addition, Huang et al. enhanced the expression levels and protein stability of MenA and MenD by co-overexpressing the MenD (A115Y) and MenA (T290M) mutants, leading to an increase in the production of MK-7 in *Bacillus subtilis* [24]. Their study indicates that mutations at the MenA and MenD loci can improve the titer of MK-7. In the MEP (2-C-methyl-D-erythritol 4-phosphate) pathway, the rate-limiting enzyme 1-deoxy-D-xylulose 5-phosphate synthase (Dxs) had two mutations: at amino acid position 60, asparagine was replaced by aspartic acid (Supplementary S1.3, Figure S2A), and at position 185, glutamine was substituted by histidine. Another rate-limiting enzyme, hydroxymethylglutaryl-CoA reductase isomerase (Dxr), had a mutation at amino acid position 315, where glutamine was substituted by lysine (Supplementary S1.3, Figure S2B). These mutations likely enhance the enzyme activity and expression of these key enzymes, increasing the metabolic flux through the MK-7 biosynthetic pathway and thereby boosting the MK-7 titer.

Table 4. Mutation status of key enzymes in the MK-7 biosynthetic pathway of *Bacillus subtilis*.

Gene Name	Base Changes	Mutation Results
Dxs	78G to A, 178A to G, 555G to T, 560T to G, 1389C to G	N60Q, Q185H
Dxr	915A to G, 11052C to A	Q351K
GlpD	None	None
MenA	586T to C, 587C to T	S196L
MenD	747 C to T, 765T to C	S249L
MenG	None	None
Fni	None	None
AroA	None	None

3.5. Overexpression of Mutant Genes Increases the Production of MK-7

To verify whether the genetic changes identified are responsible for the increased MK-7 titer in the mutant strains, this study constructed overexpression plasmids for the genes *Dxs*, *Dxr*, *menA*, and *menD* both before and after mutation. The plasmids used were pMA5-*menD*^{WT}, pMA5-*menA*^{WT}, pMA5-*Dxs*^{WT}, pMA5-*Dxr*^{WT}, pMA5-*menD*^{MT}, pMA5-*menA*^{MT}, pMA5-*Dxs*^{MT}, and pMA5-*Dxr*^{MT}. These plasmids were introduced into strain

R-8 to construct recombinant strains R-81, R-82, R-83, R-84, R-85, R-86, R-87, and R-88. Shake-flask fermentation was performed to verify the MK-7 production in these strains. As shown in Figure 8A, the results indicated that for each gene, the MK-7 titer was higher in the strains overexpressing the mutated genes compared to the wild-type genes. Specifically, R-85 had an MK-7 titer that was 19.65 mg higher than R-81; R-86 produced 20.71 mg more MK-7 than R-82; R-87 had a 17.35 mg higher MK-7 titer than R-83; and R-88 generated 16.28 mg more MK-7 than R-84. Furthermore, the mutated genes were expressed in tandem, and a pMA5-*menA-menD-Dxs-Dxr*^{MT} plasmid was constructed and introduced into strain R-8 to generate the recombinant strain R-89. The MK-7 titer in strain R-89 further increased to 239.65 mg/L (Figure 8B), which was 41.88 mg/L higher than that of the parental strain R-8. These results suggest that the amino acid mutations in the key enzymes induced by ARTP mutagenesiscan enhance enzyme activity or expression, thereby increasing the metabolic flux through the MK-7 biosynthetic pathway and leading to improved MK-7 production. The genetic stability of recombinant strains is a prerequisite for future industrial production. To verify the genetic stability of the recombinant strain R-89, the strain was continuously passaged 10 times on LB agar plates and then validated by shake-flask fermentation. Figure 8C shows that the yield of MK-7 in each generation of strain R-89 fluctuates slightly, indicating a relatively stable production and good genetic stability.

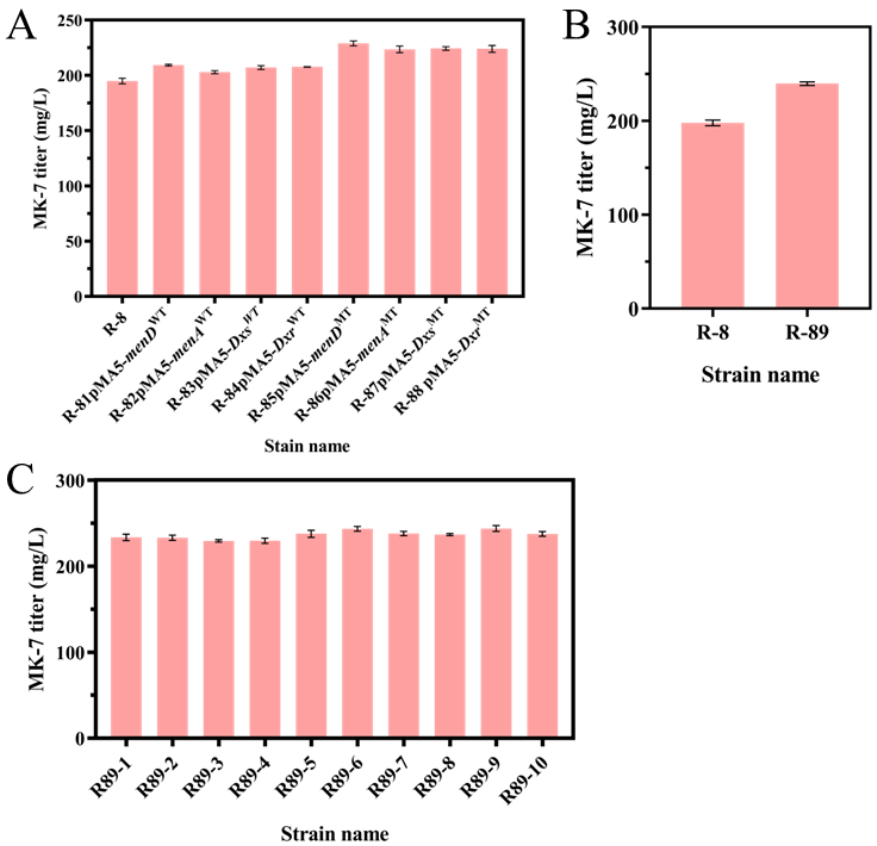


Figure 8. MK-7 production of parental strain R-8 and strains overexpressing different genes and the stability validation of the optimal recombinant strain. Each strain was fermented independently three times. (**A**) The impact of mutant genes and wild-type genes on the titer, where the maximum value of the standard deviation shown in the figure is 4.03 (mg/L). (**B**) The impact of tandem expression of four mutant genes on the titer, where the maximum value of the standard deviation shown in the figure is 2.04 (mg/L). (**C**) The genetic stability of the recombinant strain R-89, with suffixes 1, 2, 3, 4, 5, 6, 7, 8, 9, and 10 indicating the number of passages. The maximum value of the standard deviation shown in the figure is 2.92 (mg/L).

4. Conclusions

Menaquinone-7 (MK-7), as a crucial drug for the treatment of osteoporosis and cardiovascular diseases, holds significant market potential. Since the discovery of vitamin K2 in 1929, research on MK-7 has continued for nearly a century. Although previous studies have improved the titer of MK-7, it still falls short of industrial demand.

In this study, a wild strain of *Bacillus subtilis*, capable of producing MK-7, was isolated from commercially available natto fermentation agents. Shake-flask experiments confirmed that the MK-7 titer of this strain could reach 75.18 mg/L, which was designated as L-5 for subsequent experiments. This study aimed to enhance the MK-7 production capacity of L-5 by combining traditional mutagenesis and metabolic engineering techniques. Initially, using ARTP mutagenesis technology combined with protoplast technology, resistant fusion strains of HNA and DPA were obtained, and the titer was increased to 196.68 mg/L. This strain, R-8, was used for further research. To explore the genetic factors responsible for the increased MK-7 titer, whole-genome sequencing and resequencing were performed on R-8 and the parental strain L-5. This study focused on the MK-7 biosynthetic pathway and identified several mutations in key enzymes. Four mutants were found in the key enzymes of the MK-7 biosynthetic pathway, namely, MenD (S249L), MenA (S196L), Dxs (N60D, Q185H), and Dxr (T200Q). To verify whether these mutation sites are effective, overexpression plasmids for the mutants *menD* (S249L), *menA* (S196L), *Dxs* (N60D, Q185H), and *Dxr* (T200Q), as well as the wild-type *menD*, *menA*, *Dxs*, and *Dxr* from strain L-5, were constructed and introduced into strain R-8 to create recombinant strains. The results of shake-flask fermentation showed that strains overexpressing the four mutants produced higher titers of MK-7 than those overexpressing the wild-type genes from L-5, with increases of 19.65 mg, 20.71 mg, 17.35 mg, and 16.28 mg, respectively. These findings suggest that the mutations in the key enzymes' genetic loci in the MK-7 pathway are beneficial, as they likely improve enzyme activity or expression, thereby enhancing the metabolic flux of MK-7 synthesis. To further enhance the production of MK-7, the four mutants *menD* (S249L), *menA* (S196L), *Dxs* (N60D, Q185H), and *Dxr* (T200Q) were expressed in tandem. The recombinant strain R-89, expressing these genes, achieved an MK-7 titer of 239.65 mg/L, which is a significant increase in production compared to the parental strain R-8. In addition, strain R-89 also demonstrated good genetic stability. This study provides guidance and theoretical support for the future engineering of key enzymes in the MK-7 biosynthetic pathway.

Supplementary Materials: The following supporting information can be downloaded at: https://www.mdpi.com/article/10.3390/fermentation11030137/s1, Table S1. Primers used in this study. Figure S1. Mutants in the menaquinone biosynthetic pathway. (A) *menD* mutation site diagram, where F represents the wild-type strain L-5. (B) *menA* mutation site diagram, where F represents the wild-type strain L-5. Figure S2. Mutants in the MEP pathway. (A) *Dxs* mutation site diagram, where F represents the wild-type strain L-5. (B) *Dxr* mutation site diagram, where F represents the wild-type strain L-5.

Author Contributions: M.L. conducted the experiments and wrote the paper. J.L. performed the data analysis. Y.L. prepared the tables and figures. X.Z. contributed to the conception and design of the experiments. funding acquisition. J.X. All authors have read and agreed to the published version of the manuscript.

Funding: This work was supported by the Green Bio-fabrication Program of China (Grant number 2021YFC2100900), the Class I project of independent innovation of agricultural science and technology in Jiangsu Province (grant numbers CX (22) 1012), and the National Natural Science Foundation of China (Grant number 32271534).

Institutional Review Board Statement: Not applicable.

Informed Consent Statement: Not applicable.

Data Availability Statement: The original contributions presented in this study are included in the article. Further inquiries can be directed to the corresponding author.

Conflicts of Interest: The authors declare no conflicts of interest.

References

1. Fujita, Y.; Iki, M.; Tamaki, J.; Kouda, K.; Yura, A.; Kadowaki, E.; Sato, Y.; Moon, J.S.; Tomioka, K.; Okamoto, N.; et al. Association between vitamin K intake from fermented soybeans, natto, and bone mineral density in elderly Japanese men: The Fujiwara-kyo Osteoporosis Risk in Men (FORMEN) study. *Osteoporos. Int.* **2012**, *23*, 705–714. [CrossRef]
2. Azarkina, N.; Konstantinov, A.A. Stimulation of menaquinone-dependent electron transfer in the respiratory chain of *Bacillus subtilis* by membrane energization. *J. Bacteriol.* **2002**, *184*, 5339–5347. [CrossRef]
3. Theuwissen, E.; Magdeleyns, E.J.; Braam, L.A.J.L.M.; Teunissen, K.J.; Knapen, M.H.; Binnekamp, I.A.G.; van Summeren, M.J.H.; Vermeer, C. Vitamin K status in healthy volunteers. *Food Funct.* **2014**, *5*, 229–234. [CrossRef]
4. Matschiner, J.T.; Doisy, E.A., Jr. Bioassay of vitamin K in chicks. *J. Nutr.* **1966**, *90*, 97–100. [CrossRef] [PubMed]
5. Schurgers, L.J.; Teunissen, K.J.F.; Hamulyák, K.; Knapen, M.H.J.; Vik, H.; Vermeer, C. Vitamin K–containing dietary supplements: Comparison of synthetic vitamin K1 and natto-derived menaquinone-7. *Blood* **2006**, *109*, 3279–3283. [CrossRef] [PubMed]
6. Tarvainen, M.; Fabritius, M.; Yang, B.R. Determination of vitamin K composition of fermented food. *Food Chem.* **2019**, *275*, 515–522. [CrossRef] [PubMed]
7. Bentley, R.; Meganathan, R. Biosynthesis of vitamin K (menaquinone) in bacteria. *Microbiol. Rev.* **1982**, *46*, 241–280. [CrossRef] [PubMed]
8. Sato, T.; Yamada, Y.; Ohtani, Y.; Mitsui, N.; Murasawa, H.; Araki, S. Production of menaquinone (vitamin K_2)-7 by *Bacillus subtilis*. *J. Biosci. Bioeng.* **2001**, *91*, 16–20. [CrossRef]
9. Liu, K.; Fang, H.; Cui, F.; Nyabako, B.A.; Tao, T.; Zan, X.; Chen, H.; Sun, W. ARTP mutation and adaptive laboratory evolution improve probiotic performance of *Bacillus coagulans*. *Appl. Microbiol. Biotechnol.* **2020**, *104*, 6363–6373. [CrossRef] [PubMed]
10. Takahashi, I.; Ogura, K.; Seto, S. Heptaprenyl pyrophosphate synthetase from *Bacillus subtilis*. *J. Biol. Chem.* **1980**, *255*, 4539–4543. [CrossRef]
11. Tsukamoto, Y.; Kasai, M.; Kakuda, H. Construction of a *Bacillus subtilis* (*natto*) with high productivity of vitamin K_2 (menaquinone-7) by analog resistance. *Biosci. Biotechnol. Biochem.* **2001**, *65*, 2007–2015. [CrossRef] [PubMed]
12. Li, C.L.; Li, M.; Zhang, W.G.; Xu, J.Z. Accelerating the menaquinone-7 production in *Bacillus amyloliquefaciens* by optimization of the biosynthetic pathway and medium components. *Syst. Microbiol. Biomanuf.* **2023**, *3*, 776–791. [CrossRef]
13. Xu, J.Z.; Zhang, W.G. Menaquinone-7 production from maize meal hydrolysate by *Bacillus* isolates with diphenylamine and analogue resistance. *J. Zhejiang Univ. -Sci. B* **2017**, *18*, 462–473. [CrossRef] [PubMed]
14. Ma, Y.W.; McClure, D.D.; Somerville, M.V.; Proschogo, N.W.; Dehghani, F.; Kavanagh, J.M.; Coleman, N.V. Metabolic Engineering of the MEP Pathway in *Bacillus subtilis* for Increased Biosynthesis of Menaquinone-7. *ACS Synth. Biol.* **2019**, *8*, 1620–1630. [CrossRef] [PubMed]
15. Yang, S.M.; Cao, Y.X.; Sun, L.M.; Li, C.F.; Lin, X.; Cai, Z.G.; Zhang, G.; Song, H. Modular Pathway Engineering of *Bacillus subtilis* To Promote De Novo Biosynthesis of Menaquinone-7. *ACS Synth. Biol.* **2019**, *8*, 70–81. [CrossRef] [PubMed]
16. Kong, M.K.; Lee, P.C. Metabolic engineering of menaquinone-8 pathway of *Escherichia coli* as a microbial platform for vitamin K production. *Biotechnol. Bioeng.* **2011**, *108*, 1997–2002. [CrossRef] [PubMed]
17. Guerrero, R. Bergey's manuals and the classification of prokaryotes. *Int. Microbiol. Off. J. Span. Soc. Microbiol.* **2001**, *4*, 103–109. [CrossRef] [PubMed]
18. Zhang, X.; Zhang, C.; Zhou, Q.Q.; Zhang, X.F.; Wang, L.Y.; Chang, H.B.; Li, H.P.; Oda, Y.; Xing, X.H. Quantitative evaluation of DNA damage and mutation rate by atmospheric and room-temperature plasma (ARTP) and conventional mutagenesis. *Appl. Microbiol. Biotechnol.* **2015**, *99*, 5639–5646. [CrossRef]
19. Chen, L.; Chong, X.Y.; Zhang, Y.Y.; Lv, Y.Y.; Hu, Y.S. Genome shuffling of *Bacillus velezensis* for enhanced surfactin production and variation analysis. *Curr. Microbiol.* **2020**, *77*, 71–78. [CrossRef]
20. Astrup, T.; Mullertz, S. The fibrin plate method for estimating fibrinolytic activity. *Arch. Biochem. Biophys.* **1952**, *40*, 346–351. [CrossRef]
21. Cui, S.X.; Lv, X.Q.; Wu, Y.K.; Li, J.H.; Du, G.C.; Ledesma-Amaro, R.; Liu, L. Engineering a Bifunctional Phr60-Rap60-Spo0A Quorum-Sensing Molecular Switch for Dynamic Fine-Tuning of Menaquinone-7 Synthesis in *Bacillus subtilis*. *ACS Synth. Biol.* **2019**, *8*, 1826–1837. [CrossRef] [PubMed]
22. Jiang, C.; Zhao, G.; Wang, H.; Zheng, W.; Zhang, R.; Wang, L.; Zheng, Z. Comparative genomics analysis and transposon mutagenesis provides new insights into high menaquinone-7 biosynthetic potential of *Bacillus subtilis natto*. *Gene* **2024**, *907*, 148264. [CrossRef] [PubMed]

23. Min, X.; Guo, L.; Li, L.; Yang, R.; Zhao, W.; Lyu, X. Comparative transcriptome analysis reveals the underlying mechanism for over-accumulation of menaquinone-7 in *Bacillus subtilis natto* mutant. *Biochem. Eng. J.* **2021**, *174*, 108097. [CrossRef]
24. Huang, W.; Li, J.; Zhu, Q.; Lv, J.; Zhu, R.; Pu, C.; Zhao Hua, B.; Fu, G.; Zhang, D. Increasing Vitamin K_2 Synthesis in *Bacillus subtilis* by Controlling the Expression of MenD and Stabilizing MenA. *J. Agric. Food Chem.* **2024**, *72*, 22672–22681. [CrossRef] [PubMed]
25. Li, C.; Wang, H.; Wang, L.; Wang, P.; Zheng, Z. Enhancement of MK-7 synthesis by engineered strains of *Bacillus subtilis natto* that overexpress men genes and by increasing available dissolved oxygen. *Chin. J. Appl. Environ. Biol.* **2022**, *28*, 1393–1399. [CrossRef]
26. Ding, X.; Zheng, Z.; Zhao, G.; Wang, L.; Wang, H.; Yang, Q.; Zhang, M.; Li, L.; Wang, P. Bottom-up synthetic biology approach for improving the efficiency of menaquinone-7 synthesis in *Bacillus subtilis*. *Microb. Cell Factories* **2022**, *21*, 101. [CrossRef] [PubMed]
27. Liu, Y.; Ding, X.-M.; Xue, Z.-L.; Hu, L.-X.; Cheng, Q.; Chen, M.-H.; Su, Y.; Zhu, B.; Xu, P. Site-directed mutagenesis of UbiA to promote menaquinone biosynthesis in *Elizabethkingia meningoseptica*. *Process Biochem.* **2017**, *58*, 186–192. [CrossRef]

Disclaimer/Publisher's Note: The statements, opinions and data contained in all publications are solely those of the individual author(s) and contributor(s) and not of MDPI and/or the editor(s). MDPI and/or the editor(s) disclaim responsibility for any injury to people or property resulting from any ideas, methods, instructions or products referred to in the content.